Fidelity of CMIP5 models in simulating the observed Interdecadal Pacific Oscillation and Indian Summer Monsoon Rainfall Teleconnection

Dr. Manish Kumar Joshi
(IITM, CCCR Division, India)
&
Dr. Fred Kucharski
(ICTP, Trieste, Italy)

Outline

- Introduction
- Motivation
- Objectives
- Methodology
- Results
- Conclusion

Introduction

- The climate system shows various modes of variability.
- The natural internal variability on D2M timescales in the Pacific as well as in the extratropical North Atlantic Oceans extremely affects the climate of India.
  - This raises the possibility that the regional SST variability of the Pacific and the extratropical North Atlantic may provide supplementary information that will improve monsoon predictions over India.
- Successful simulation and prediction of these modes increase confidence in the CGCMs used for climate predictions.
- Therefore, it is essential to see whether the models are capable of simulating these modes or not.

Motivation

- The warm (cold) phase of IPO-like variability observed in SST of the North Pacific Ocean is associated with deficit (excess) of rainfall over India [*Krishnamurthy & Krishnamurthy*, 2014]
- The opposite phases of AMO and IPO together influences the rainfall over WC and NE regions in an asymmetric manner [*Joshi & Rai,* 2015]

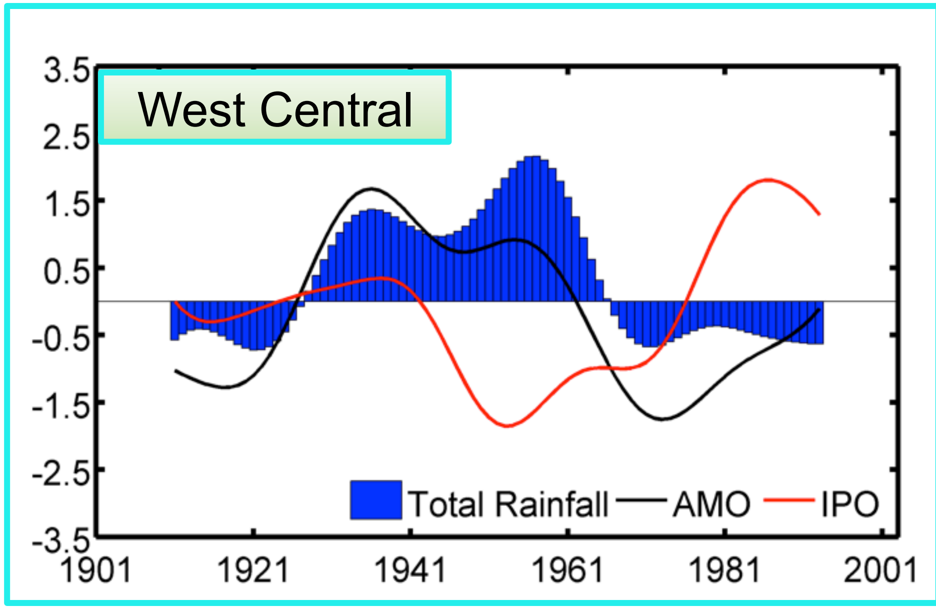

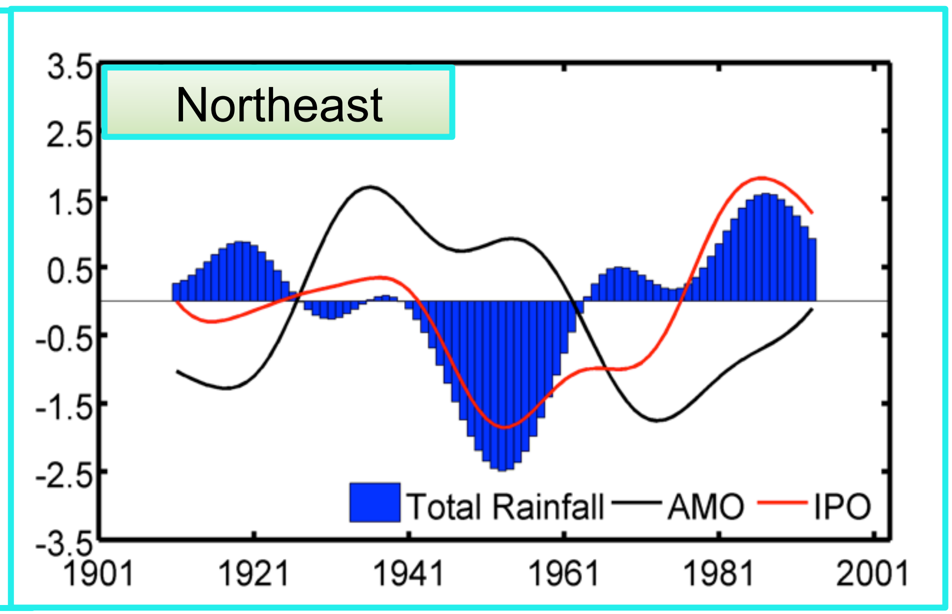

Clim Dyn
DOI 10.1007/s00382-016-3210-8

Current Research Work

CrossMark

Impact of Interdecadal Pacific Oscillation on Indian summer monsoon rainfall: an assessment from CMIP5 climate models

Manish K. Joshi[1] · Fred Kucharski[2,3]

Published in Climate Dynamics

Objectives

- To evaluate the fidelity of 32 CMIP5 models in simulating IPO-ISMR teleconnection.
- This study addresses the following issues:
  - Are the CMIP5 models under consideration capable of simulating IPO?
  - Do the CMIP5 models have capability to reproduce the IPO-ISMR teleconnection?
  - Is there any relationship between the quality of reproducing IPO and IPO-ISMR teleconnection in the models?
  - Are the CMIP5 models capable of reproducing the atmospheric circulation and the convergence/divergence patterns associated with the IPO?

Model	Institution	Resolution (Latitude x Longitude)
BCC-CSM1-1	Beijing Climate Center, China Meteorological Administration, China	64 x 128
BCC-CSM1-1-m	Beijing Climate Center, China Meteorological Administration, China	160 x 320
BNU-ESM	College of Global Change and Earth System Science, Beijing Normal University, China	64 x 128
CCSM4	National Center for Atmospheric Research, USA	192 x 288
CMCC-CESM	Centro Euro-Mediterraneo per I Cambiamenti Climatici, Italy	48 x 96
CMCC-CMS	Centro Euro-Mediterraneo per I Cambiamenti Climatici, Italy	96 x 192
CanCM4	Canadian Centre for Climate Modelling and Analysis, Canada	64 x 128
CanESM2	Canadian Centre for Climate Modelling and Analysis, Canada	64 x 128
GFDL-CM3	Geophysical Fluid Dynamics Laboratory, USA	90 x 144
GFDL-ESM2G	Geophysical Fluid Dynamics Laboratory, USA	90 x 144
GFDL-ESM2M	Geophysical Fluid Dynamics Laboratory, USA	90 x 144
GISS-E2-H	NASA Goddard Institute for Space Studies, NY	90 x 144
GISS-E2-R	NASA Goddard Institute for Space Studies, NY	90 x 144
HadCM3	Met Office Hadley Centre, UK	73 x 96
HadGEM2-AO	National Institute of Meteorological Research/Korea Meteorological Administration, South Korea	145 x 192
HadGEM2-CC	Met Office Hadley Centre, UK	145 x 192
HadGEM2-ES	Met Office Hadley Centre, UK	145 x 192
INM-CM4	Institute for Numerical Mathematics, Russia	120 x 180
IPSL-CM5A-LR	Institut Pierre-Simon Laplace, France	96 x 96
IPSL-CM5A-MR	Institut Pierre-Simon Laplace, France	143 x 144
IPSL-CM5B-LR	Institut Pierre-Simon Laplace, France	96 x 96
MIROC4h	Atmosphere and Ocean Research Institute (The University of Tokyo), National Institute for Environmental Studies, and Japan Agency for Marine-Earth Science and Technology, Japan	320 x 640
MIROC5	Atmosphere and Ocean Research Institute (The University of Tokyo), National Institute for Environmental Studies, and Japan Agency for Marine-Earth Science and Technology, Japan	128 x 256
MIROC-ESM	Japan Agency for Marine-Earth Science and Technology, Atmosphere and Ocean Research Institute (The University of Tokyo), and National Institute for Environmental Studies, Japan	64 x 128
MIROC-ESM-CHEM	Japan Agency for Marine-Earth Science and Technology, Atmosphere and Ocean Research Institute (The University of Tokyo), and National Institute for Environmental Studies, Japan	64 x 128
MPI-ESM-LR	Max Planck Institute for Meteorology (MPI-M), Germany	96 x 192
MPI-ESM-MR	Max Planck Institute for Meteorology (MPI-M), Germany	96 x 192
MPI-ESM-P	Max Planck Institute for Meteorology (MPI-M), Germany	96 x 192
MRI-CGCM3	Meteorological Research Institute, Japan	160 x 320
MRI-ESM1	Meteorological Research Institute, Japan	160 x 320
NorESM1-M	Norwegian Climate Centre, Norway	96 x 144
NorESM1-ME	Norwegian Climate Centre, Norway	96 x 144

Table List of CMIP5 models along with their modeling groups and resolution

Methodology

- The "horse-shoe" shape of this EOF exhibits ENSO-like SST patterns in the Pacific basin and PDO like SST patterns in the North Pacific,
  - Suggests that PDO is a part of IPO that extends to the whole Pacific basin.
- PC-1 contains both ENSO-related multi-year variations & D2M variations.
- Since the focus of the present study is to examine the IPO-ISMR teleconnection on multidecadal basis, the obtained unfiltered IPO index is filtered using Butterworth LPF of order 4 and cut-off frequency 21-year (shown by red line).
- The LPF IPO indices for the forced simulations are also derived using the same methodology as discussed above.

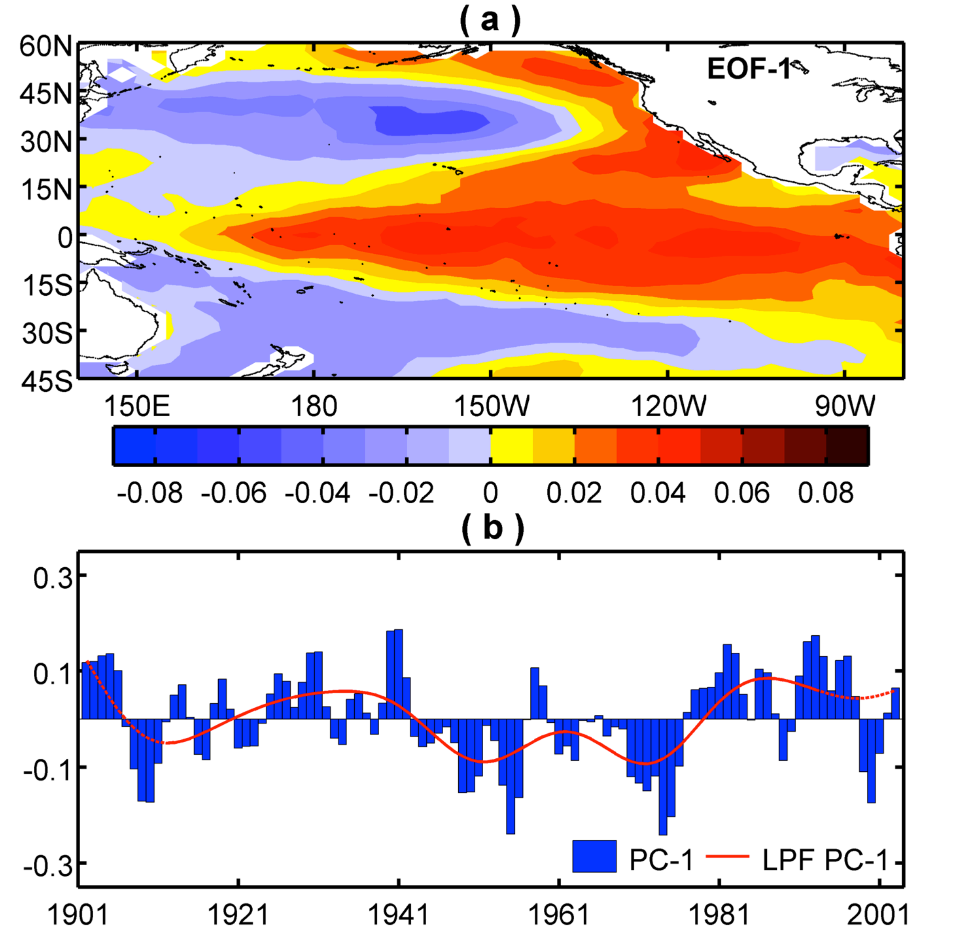

Fig. First EOF of the detrended smoothed (3-year moving average) annual mean SSTAs computed over the Pacific basin (45°S to 60°N, 140°E to 80°W) and **b** its associated PC-1, i.e., unfiltered IPO (shown by blue bars) and red curve is a smoothed time series obtained by applying Butterworth LPF (order 4, cut-off frequency 21-year) to unfiltered IPO. The first and last 10-points of the filtered time series are ignored due to end effects of LPF (shown by dashed line).

Joshi & Kucharski, *Clim. Dynam.*, 2016

Precipitation Simulation

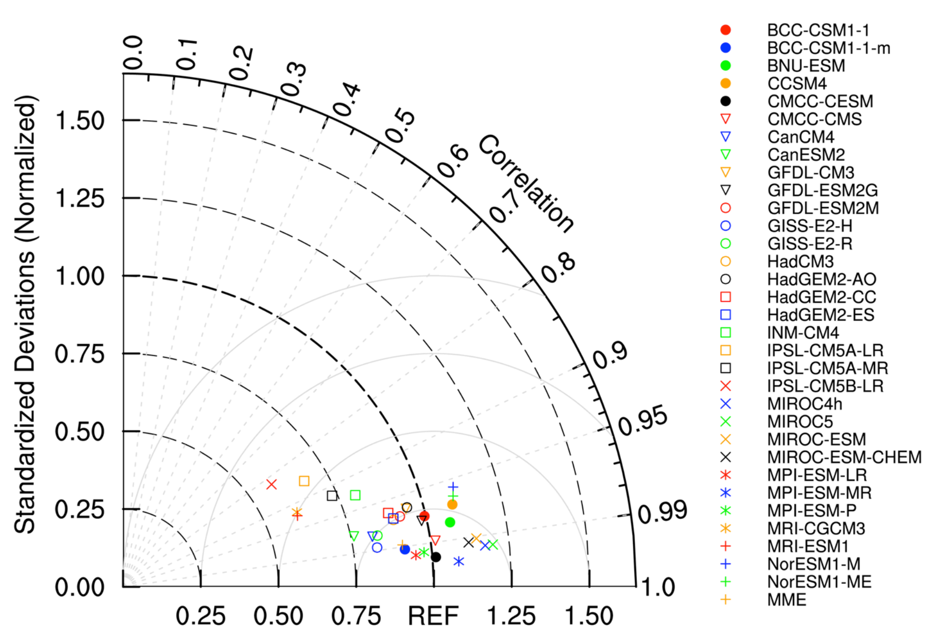

Fig. Annual cycle, representing the climatological monthly mean of precipitation area-averaged over the monsoon core region (10°N to 30°N, 70°E to 100°E).

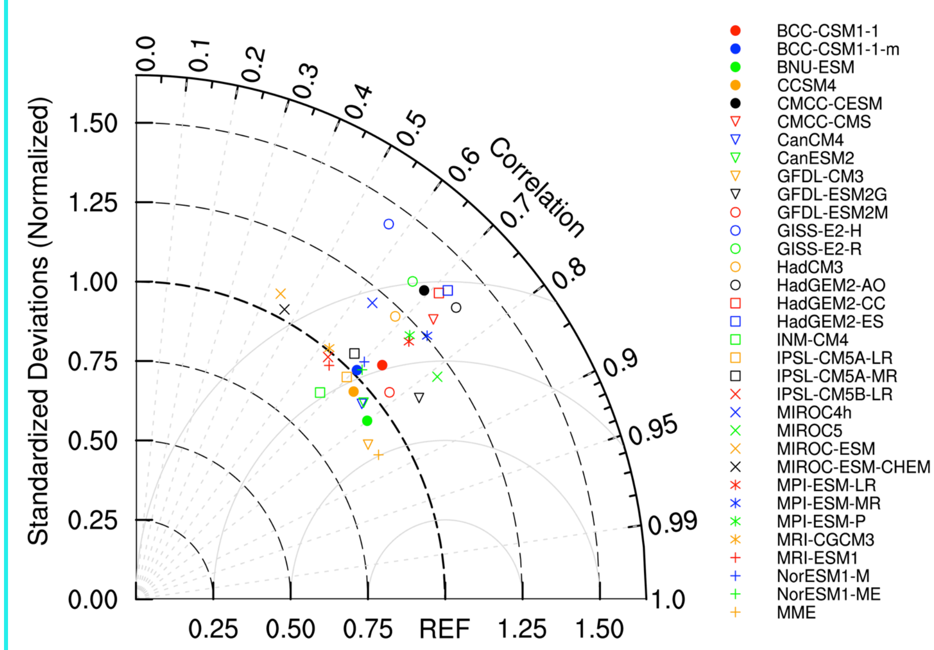

Fig. Spatial pattern of climatological seasonal (JJAS) mean precipitation over the Indian monsoon region (15°S to 30°N, 50°E to 120°E).

- Except IPSL-CM5B-LR and IPSL-CM5A-LR, all other models show a CC > 0.9.
- But, some either underestimate or overestimate the variance.
- In terms of both magnitude and phase, the models BCC-CSM1-1, CMCC-CESM, CMCC-CMS, GFDL-ESM2G, MPI-ESM-LR, MPI-ESM-MR, and MPI-ESM-P are very close to the observation and hence, simulate the best annual cycle as compared to other models.

- Most of the models show good CCs.
- Criteria to identify models: CC > 0.6 and normalized SD lying between 0.75 and 1.25.
- Based on this criterion, the models MIROC-ESM and MIROC-ESM-CHEM have lowest CC, while the models GISS-E2-H, GISS-E2-R, CMCC-CESM, CMCC-CMS, HadGEM2-AO, HadGEM2-CC, HadGEM2-ES, and MPI-ESM-MR are highly overestimating the climatological seasonal mean precipitation.

Joshi & Kucharski, *Clim. Dynam.*, 2016

- Models are not selected based on the above criterion for the analysis of IPO-ISMR teleconnection, because all models are to some extent able to reproduce the:
  - ISMR seasonal cycle and
  - Climatology
- Also, a selection would involve the risk of excluding models from further analysis because of ad-hoc and subjectively chosen thresholds.

Joshi & Kucharski, *Clim. Dynam.*, 2016

IPO Simulation

Fig. Regression maps of annual SSTAs onto the standardized LPF IPO index for observation and 32 CMIP5 models. The grey contours in observation and CMIP5 models indicate the regions where the regression coefficient is statistically significant at 95% CL, which is assessed via a two-tailed t test.

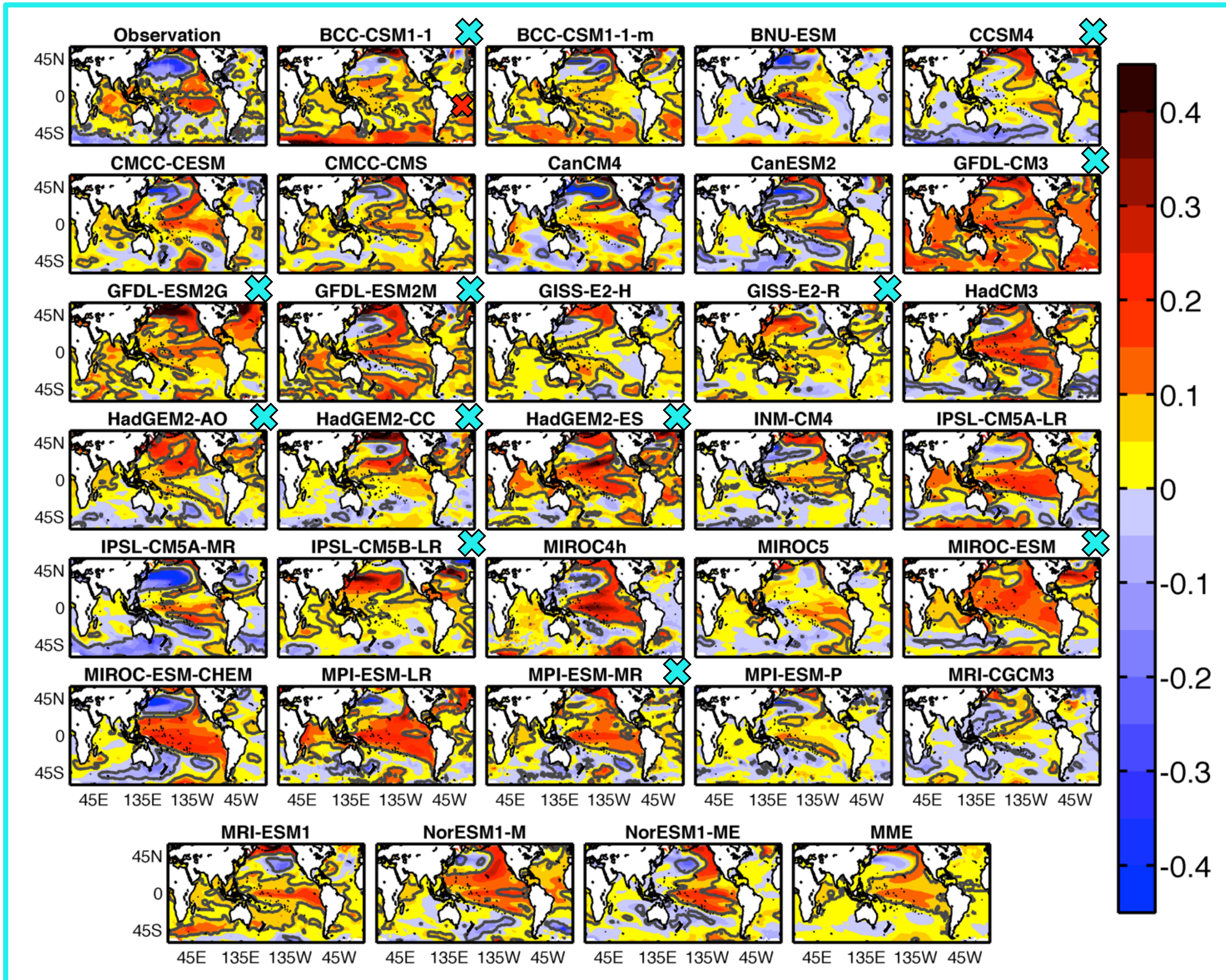

Joshi & Kucharski, *Clim. Dynam.*, 2016

IPO-ISMR Teleconnection

✧ Positive phase of IPO causes:

- Reduction of rainfall: - all-India
- Enhancement of rainfall: - NE Region

✧ Most of the models show -ve anomalies over all-India as seen in observations, except the ones shown by cross.

✧ Models that fail to reproduce the IPO-ISMR teleconnection are the ones that are also showing a poor spatial pattern of IPO.

✧ The models BNU-ESM, CanCM4, CanESM2, MIROC4h, and NorESM1-M show the best regression pattern as seen in the observation.

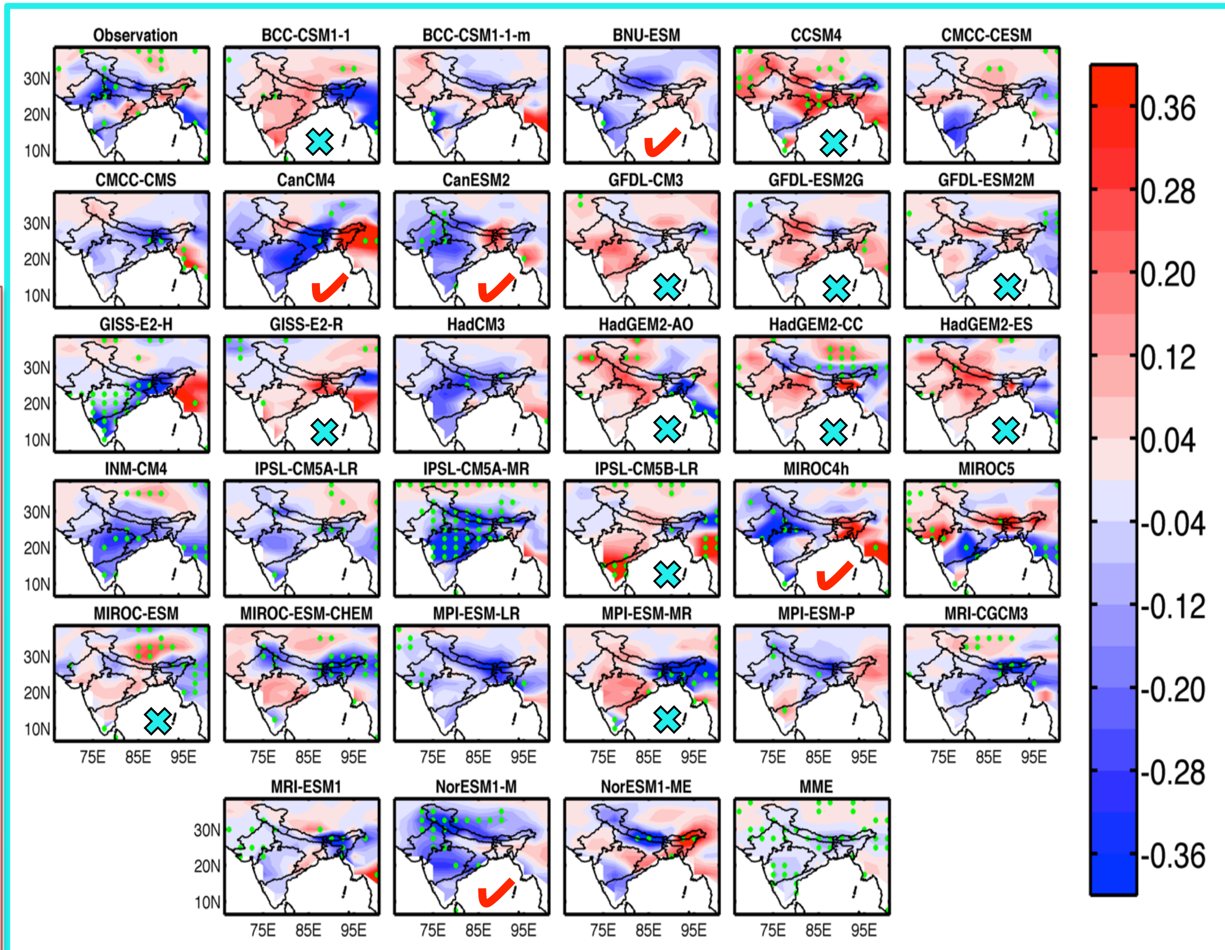

Fig. Regression maps of JJAS precipitation anomalies onto the standardized LPF IPO index (units are mm/d per standard deviation) for observation and 32 CMIP5 models. The green stippling in observation and CMIP5 models indicates the grid point where the regression coefficient is statistically significant at 90% CL, which is assessed via a two-tailed t test.

Joshi & Kucharski, *Clim. Dynam.*, 2016

Categorization of Models

- Based on the sign of average regression coefficients, the models are categorized into two groups:
  - Good (-ve) &
  - Poor (+ve).
- The ensemble mean of good models closely resembles to the observation.

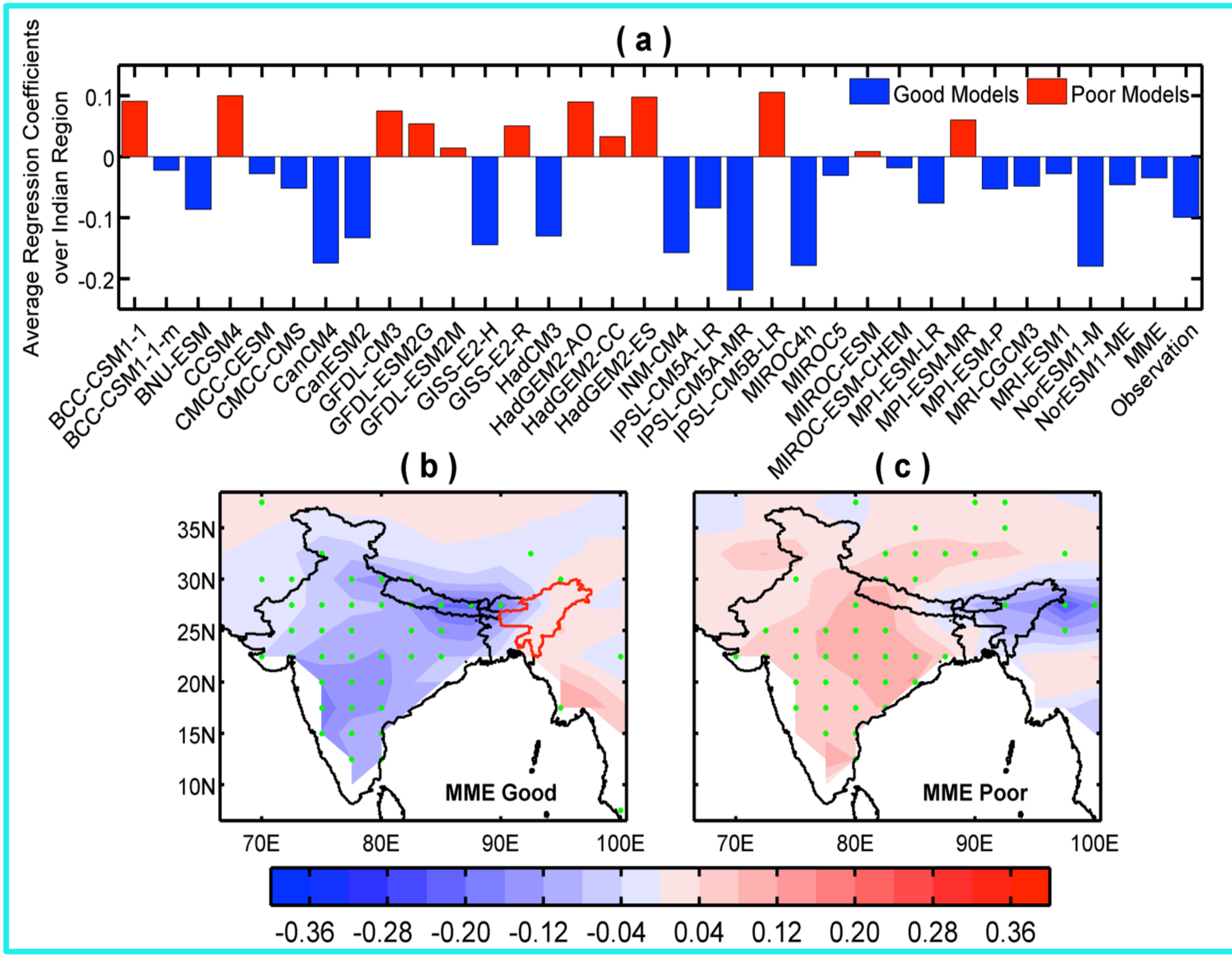

Fig. a Area average of the IPO precipitation regression maps over Indian land points, excluding northeast region. **b** and **c** Ensemble means of the IPO precipitation regression patterns of 20 good (MME good) and 12 poor (MME poor) CMIP5 models, respectively. The green stippling in MME good and MME poor indicates the grid point where the sign of regression coefficient coincides in at least 15 out of the 20 good and 9 out of the 12 poor models, respectively.

Joshi & Kucharski, *Clim. Dynam.*, 2016

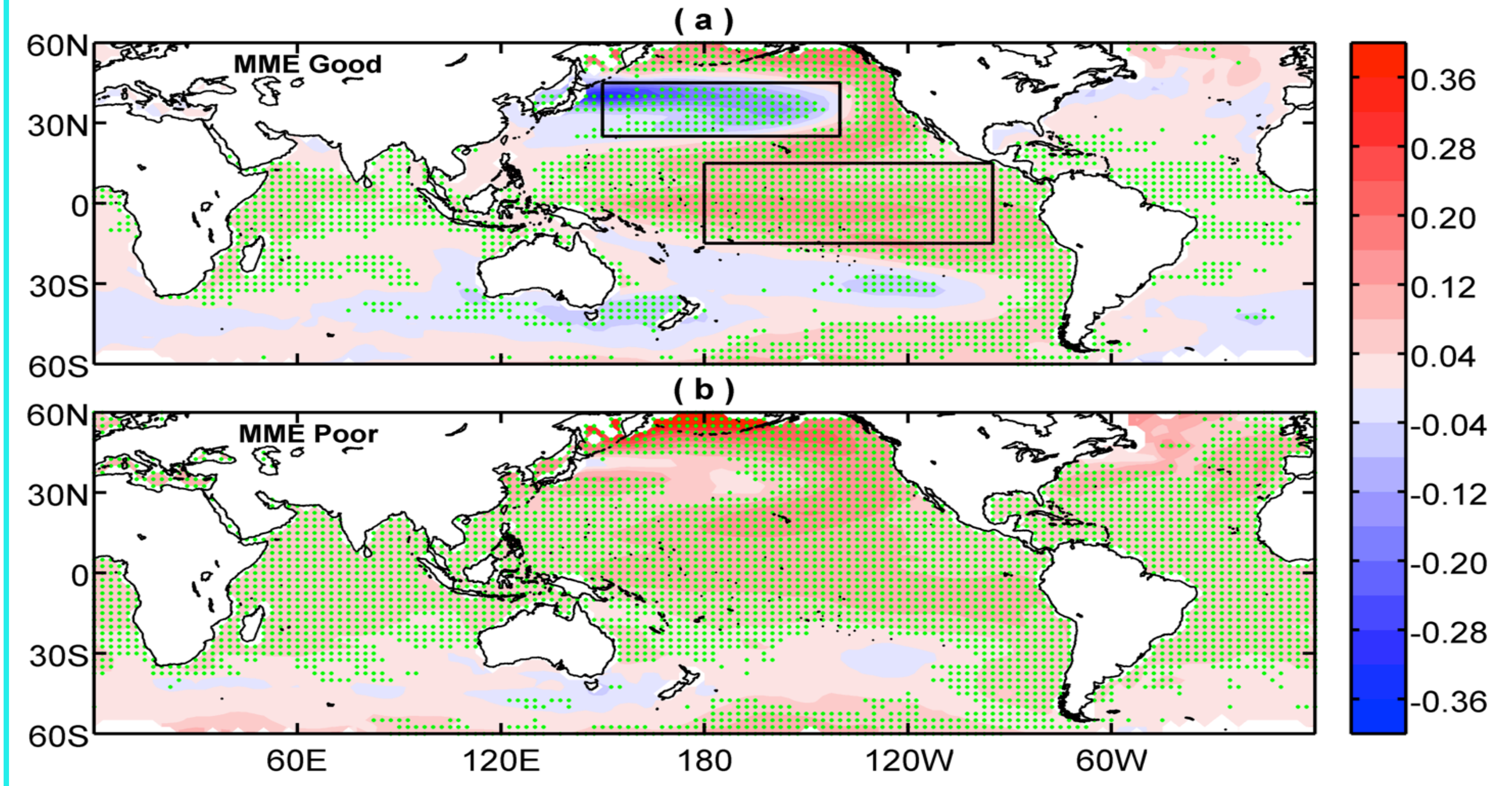

- In order to get further insight of the crucial elements in the model IPO pattern the ensemble means of good and poor models constructed.
- As compared to poor models, the composite of good models shows pronounced tropical-extratropical SST gradient, which compares well with the observations.

Fig. Ensemble means of the IPO SST regressions of **a** good (MME good) and **b** poor (MME poor) CMIP5 models, which are computed by averaging the regression maps of annual SSTAs onto the standardized LPF IPO index across all 20 good and 12 poor models. The green stippling in MME good and MME poor indicates the grid point where the sign of regression coefficient coincides in at least 15 out of the 20 good and 9 out of the 12 poor models, respectively..

Joshi & Kucharski, *Clim. Dynam.*, 2016

Fig. Scatter plot of the IPO precipitation regressions averaged over Indian land points, excluding northeast region versus the difference between mean IPO SST regressions over **a** the tropical (15°S to 15°N, 180°E to 95°W) and extratropical (25°N to 45°N, 150°E to 140°W) Pacific Ocean and **b** the Niño 3.4 (5°S to 5°N, 120°W to 170°W) region and Indian Ocean (10°S to 10°N, 60°E to 90°E).

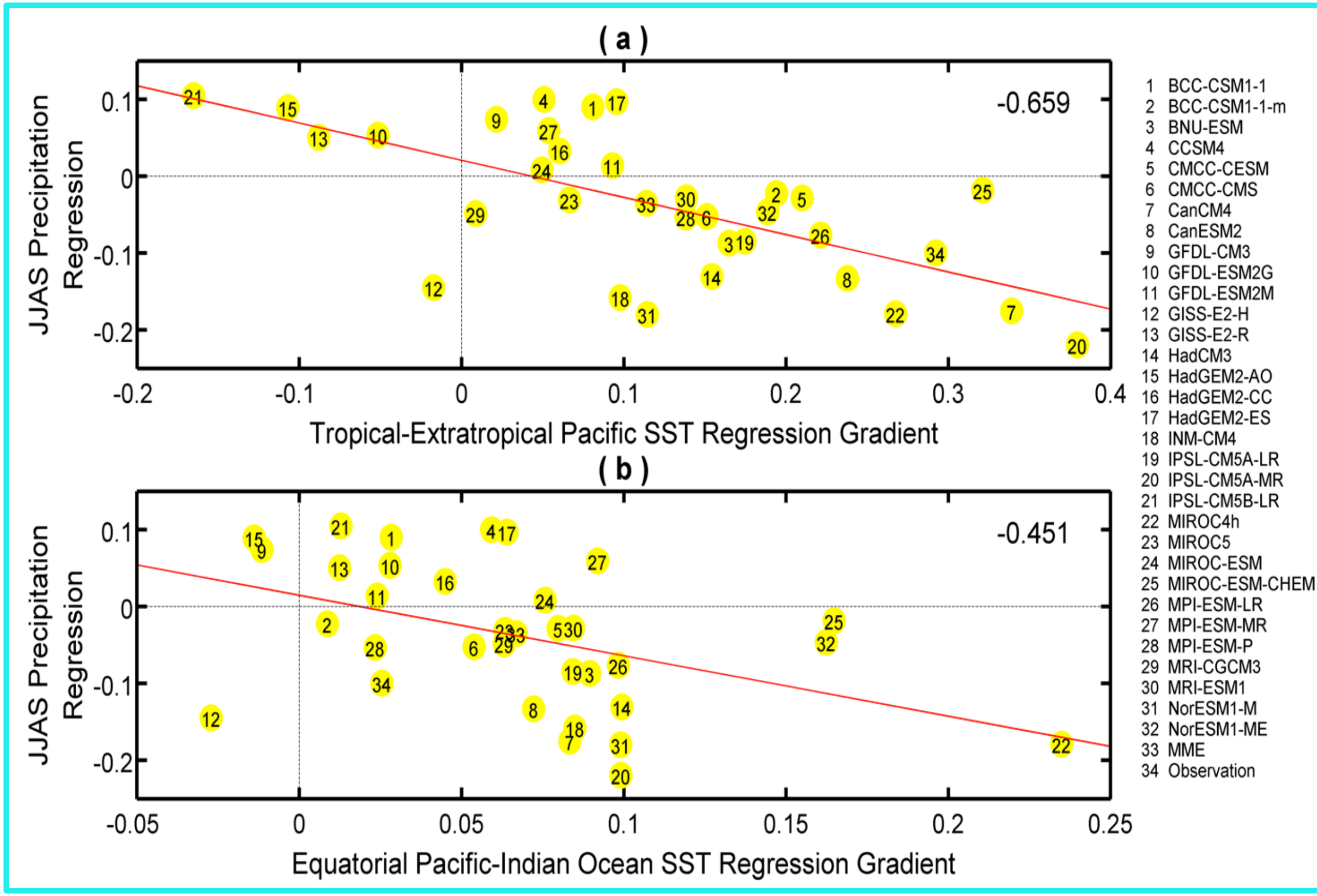

✧ Strong relationship between the quality of reproducing the IPO pattern and the IPO-ISMR teleconnection in models.

Joshi & Kucharski, *Clim. Dynam.*, 2016

Capability of CMIP5 models in reproducing the Atmospheric Circulation and the Convergence/Divergence patterns associated with the IPO

- The warm phase of IPO is associated with westerly anomalies along the equator.
- The winds are blowing away from the continent:
  - Indicating the lack of moisture flow over India, which is consistent with less rainfall.

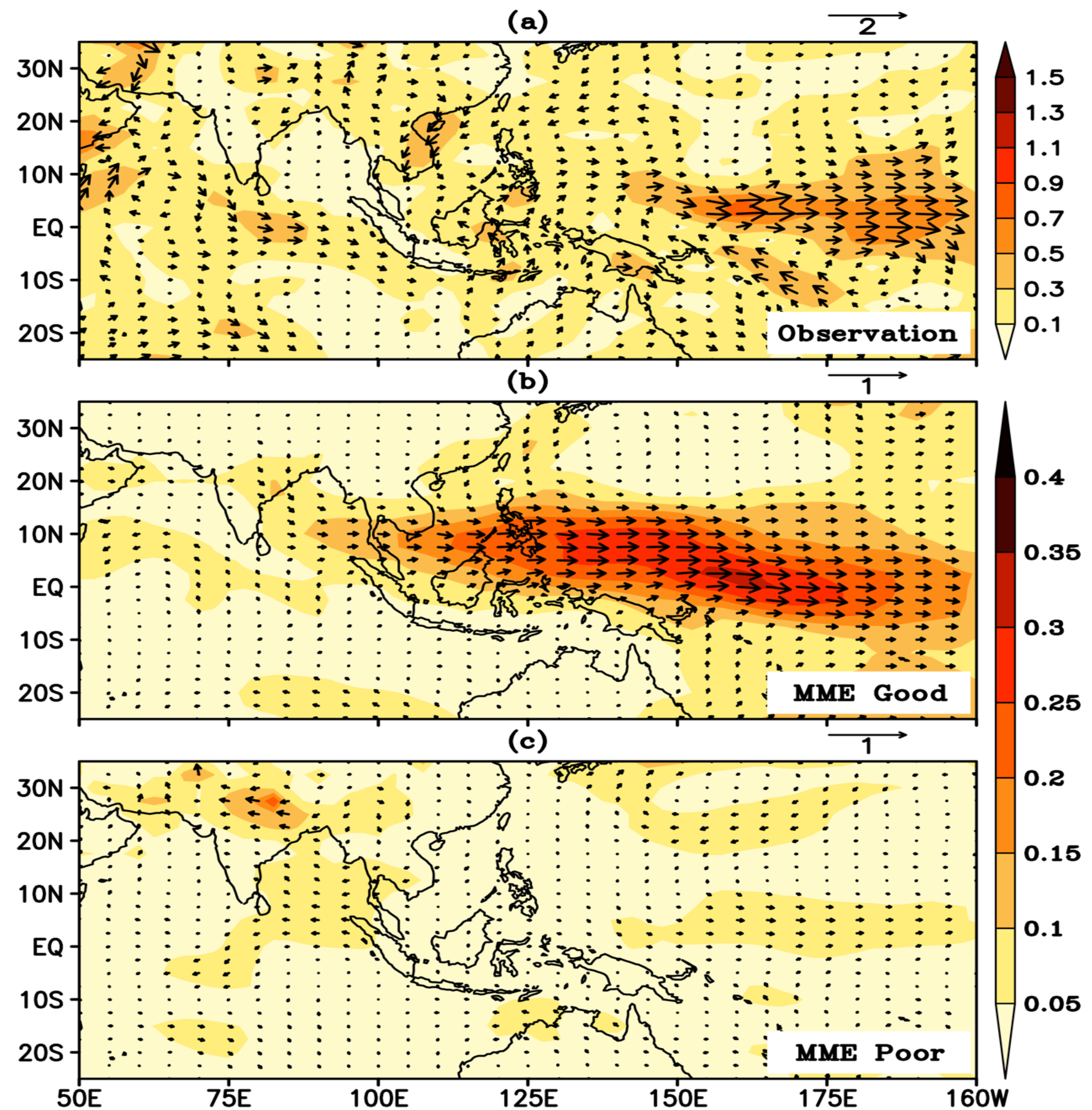

Fig. a Regression of JJAS seasonal anomalies of zonal and meridional winds at 850 hPa from NCEP/NCAR reanalysis (1948–1993) onto the standardized LPF IPO index. **b** and **c** Same as in Fig. a, but for the averaged regressions of 20 good and 12 poor CMIP5 models, respectively. Magnitude of winds is represented by shaded color and vectors represent wind direction.

Joshi & Kucharski, *Clim. Dynam.*, 2016

✧ The warm phase of IPO is associated:

- Anomalous convergence: central tropical Pacific & Southwest US.
- Divergence over West Africa and extended Indian monsoon region at low levels.
- With anomalous divergence and convergence over the respective regions at high levels.

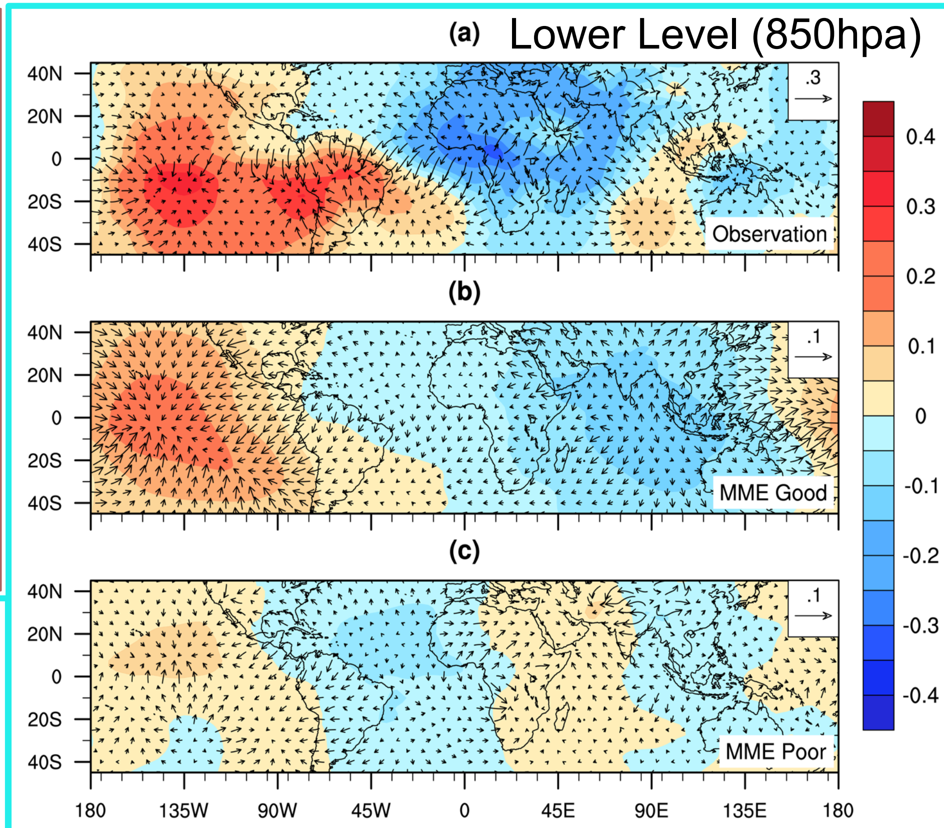

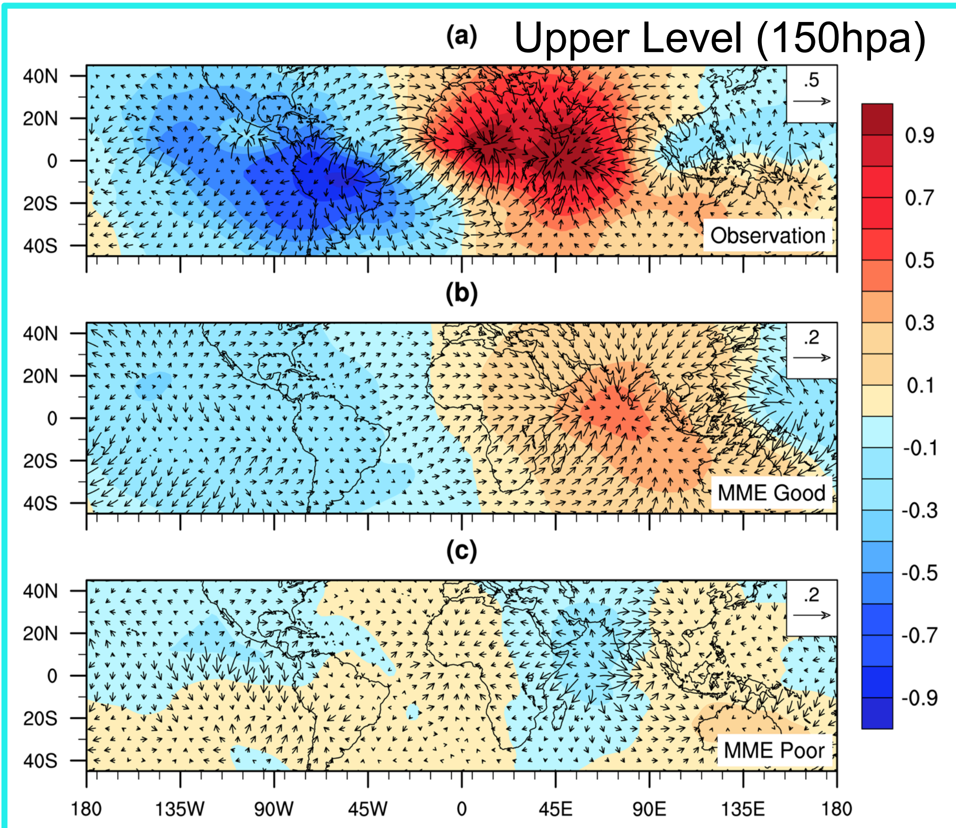

Fig. a Regression of JJAS anomaly of velocity potential at 850 hPa (150hPa) from NCEP/NCAR reanalysis (1948–1993) onto the standardized LPF IPO index. **b** and **c** Same as in Fig. a, but for the averaged regressions of 20 good and 12 poor CMIP5 models, respectively. The unit of velocity potential is 10^6 m^2/s per standard deviation. The vectors represent the divergent wind (m/s).

Joshi & Kucharski, *Clim. Dynam.*, 2016

Possible Physical Mechanism – Related to the modification of Walker Circulation

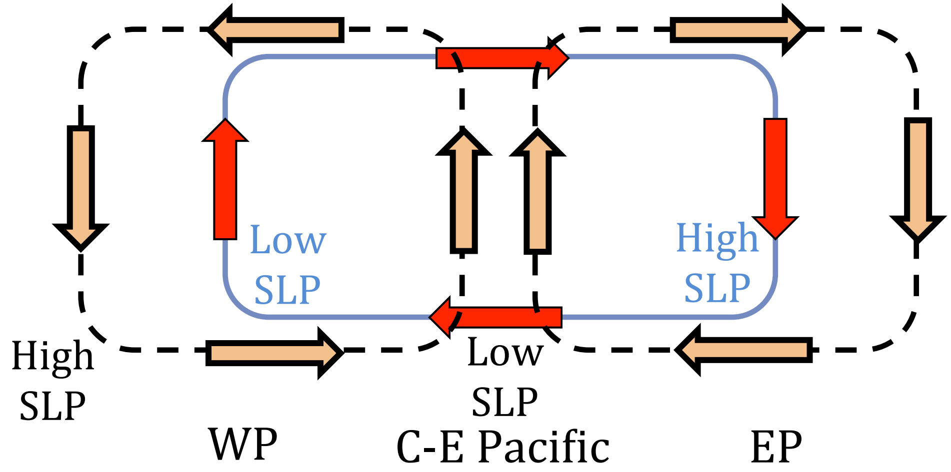

Zonal Over Turning Circulation

Anomalous Walker Circulation

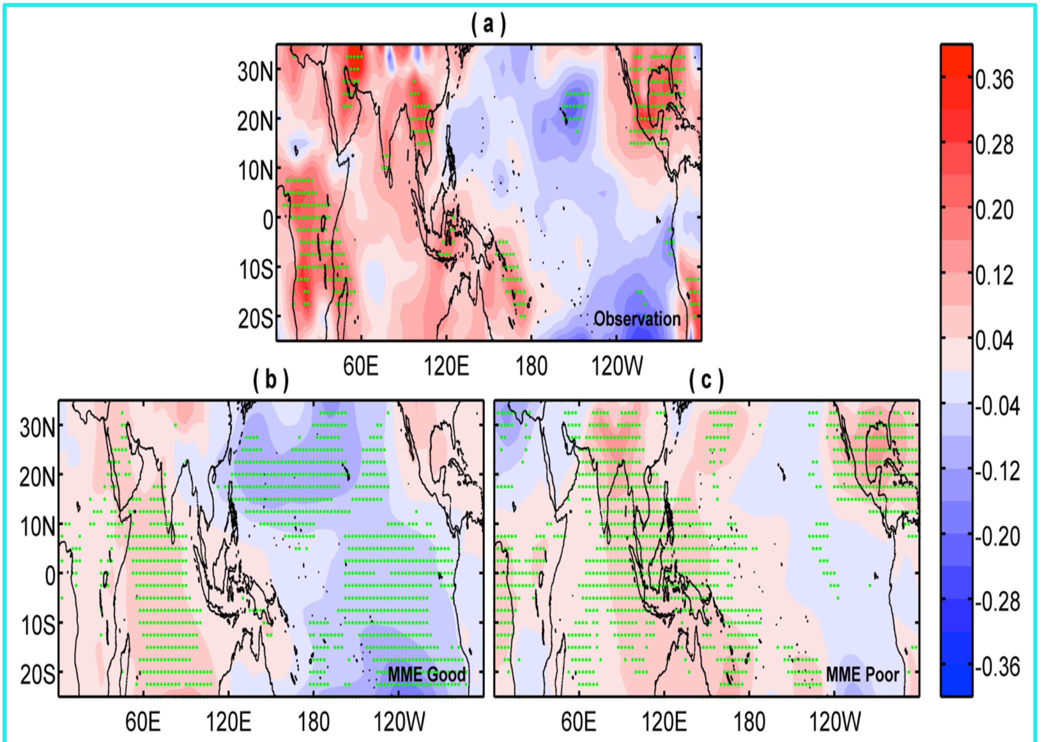

- ✧ This mechanism can also be verified through IPO-SLP regressions.
- ✧ As compared to good models, the ensemble mean of poor models fails to reproduce the IPO SLP regression pattern over the tropical Pacific.

Fig. a Regression of JJAS seasonal anomaly of SLP from NCEP/NCAR reanalysis (1948–1993) onto the standardized LPF IPO index. **b** and **c** Same as in Fig. a, but for the averaged regressions of 20 good and 12 poor CMIP5 models, respectively.

Joshi & Kucharski, *Clim. Dynam.*, 2016

Conclusion

- Two-thirds of the models show well-defined spatial pattern of IPO and most amongst these capture the IPO-ISMR teleconnection.

- Models that fail to reproduce IPO-ISMR teleconnection:
  - Are the ones that are showing a poor spatial pattern of IPO, irrespective of the extent to which they reproduce the precipitation climatology and seasonal cycle.

- The results reveal a strong relationship between the quality of reproducing the IPO pattern and the IPO-ISMR teleconnection in the models:
  - In particular with respect to the tropical-extratropical as well as the equatorial Pacific-Indian Ocean SST gradients during IPO phases.

- Models reproducing IPO-ISMR teleconnection
  - Also reasonably simulate the atmospheric features.

- The physical mechanism for IPO-ISMR teleconnection is related to a modification of the Walker circulation.

Thank You